DOI: 10.1002/anie.200700303

Improved Designs of Metal–Organic Frameworks for Hydrogen Storage**

*Sang Soo Han, Wei-Qiao Deng, and William A. Goddard, III**

Hydrogen fuel is considered as a most promising alternative energy source for vehicles and portable electronics.[1] For this technology to be practical for automobiles, the U.S. Department of Energy has established a design target of 6.0 wt% reversible hydrogen storage by 2010, but current materials fall far short of this goal. Consequently, many studies are devoted to metal hydride[2,3] and carbon-based materials.[4–8] Furthermore, such novel concepts as BN nanotubes,[9,10] clathrate hydrates,[11] and metal–organic frameworks (MOFs)[12–25] are being pursued.

In particular MOF materials have attracted attention because of their relatively simple and economic synthesis (compared with chemical vapor deposition), large storage amounts (1.32 wt% hydrogen was reported at 1 bar and 77 K), and high thermal stability up to 400 °C.[12,20] To provide a fundamental understanding of storage mechanisms and to determine the optimum performance for such MOFs, we report herein first-principles-based calculations on a variety of MOFs.

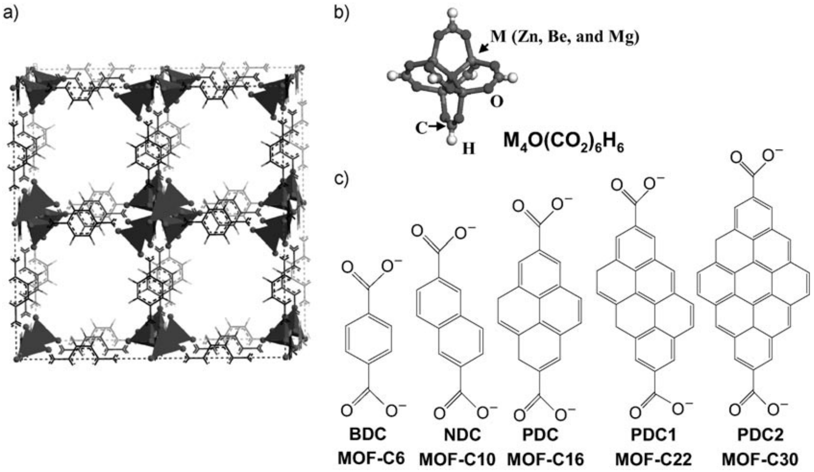

Figure 1. Atomistic structures of MOFs. An overview of the complete structure is shown in (a), where the purple tetrahedra correspond to the metallic nodes in (b). The different linkers are shown in (c).

Figure 1 shows the atomistic structures of several MOFs. The $M_4O(CO_2)_6$ cluster (where M = Zn, Be, or Mg) serves as a metal oxide node that links organic aromatic units (such as benzene or dibenzo coronene) to form a cubic cage structure.

We consider two strategies to enhance the hydrogen storage of MOFs:

a) Optimize the metal oxide nodes by using alternative lighter metal elements. We consider replacing M = Zn with Be or Mg.
b) Optimize the organic linker to enhance the hydrogen adsorption energy. We consider five organic linkers: BDC (MOF-C6), NDC (MOF-C10), PDC (MOF-C16), PDC1 (MOF-C22), and PDC2 (MOF-C30), where the MOFs are named according to the number of aromatic carbon atoms in the linker.

To determine a force field that accurately predicts the interaction of H_2 with the organic linkers, we carried out quantum mechanics (QM) calculations for H_2/benzene and H_2/naphthalene (RI-MP2/TZVPP[26]) and for H_2 bound to the $OM_4O_{12}(CH)_6$ cluster in Figure 1 b for M = Be, Mg, and Zn (RI-MP2/QZVPP[26]). The results are summarized in Table 1. The Mg-based cluster has a higher adsorption energy for H_2 than the Zn-based cluster, but a slightly lower energy is found for the Be case. Moreover, we find that the binding of H_2 to

Table 1: Interaction energies ($kJ\,mol^{-1}$) of hydrogen molecules with metal oxide nodes and organic linkers.

Method	$H_2\cdots C_6H_6$	$H_2\cdots C_{10}H_8$	$H_2\cdots$ Zn node	$H_2\cdots$ Mg node	$H_2\cdots$ Be node
RI-MP2	−3.81	−4.27	−6.24	−6.78	−4.40
FF	−3.81	−4.27	−6.20	−6.70	−4.48

---

[*] Dr. S. S. Han, Prof. W.-Q. Deng,[+] Prof. W. A. Goddard, III
Materials and Process Simulation Center
California Institute of Technology
Pasadena, CA 91125 (USA)
Fax: (+1) 626-585-0918
E-mail: wag@wag.caltech.edu

[+] Current address:
Nanyang Technology University
Singapore (Singapore)

[**] The facilities of the Materials and Process Simulation Center were supported by ONR-DURIP and ARO-DURIP. Additional support of the MSC was provided by MURI-ARO, MURI-ONR, DOE (ASC, FETL), NSF (NIRT), NIH, Boehringer-Ingelheim, Chevron, Dow-Corning, Intel, Nissan, and Pfizer. This research was partially supported by a grant from the DOE (DE-FG01-04ER04-20). Also, S.S.H. was partially supported by the Korean Research Foundation Grant funded by the Korean Government (MOEHRD) (KRF-2005-214-D00303). We thank Prof. Omar Yaghi (UCLA) for helpful comments.

Supporting information for this article is available on the WWW under http://www.angewandte.org or from the author.

the metal oxide clusters is stronger than with aromatic rings, such as benzene and naphthalene. This phenomenon validates the suggestion in references [27–30] that the most favored adsorption sites are at the metallic nodes.

Next, we developed new van der Waals parameters for H to C, H, O, and M that fit the QM results (see the Supporting Information). As shown in Table 1, the new force field (FF) leads to an excellent description of the van der Waals interactions between H_2 gas and the metal and aromatic units.

In fact, there are ab initio studies on an accurate interaction of H_2 with various organic linkers and with an $OZn_4O_{12}(CH)_6$ cluster.[31–33] Sagara et al. reported with RI-MP2/QZVPP (the same method as our calculations) that the binding energy of H_2 with $OZn_4O_{12}(CH)_6$ is 6.28 kJ mol^{-1}, which is very close to our result (6.24 kJ mol^{-1}).[31] And higher-level MP2 calculations than our RI-MP2/TZVPP indicate an H_2 binding energy that is approximately 1 kJ mol^{-1} higher with organic linkers.[31,33] However, as explained below, our FF developed from RI-MP2/Q(T)ZVPP accurately predicts the H_2 uptake capacity of MOF systems, thus demonstrating that our FF is reasonable.

Using this first-principles-derived force field in conjunction with grand canonical Monte Carlo (GCMC) simulations,[34,37] we calculated hydrogen uptake in the three-dimensional MOF crystal structures to obtain the average loading of hydrogen molecules at various pressures and temperatures. To eliminate boundary effects, we used an infinite three-dimensionally periodic cell containing four independent sheets, each with 32 metal atoms. Additional calculation details are included in the Supporting Information.

We now focus on optimizing the cubic MOF structures (IRMOF types). Lattice parameters of the Zn-MOFs simulated in this work are 26.025 (MOF-C6), 30.252 (MOF-C10), 34.374 (MOF-C16), 38.652 (MOF-C22), and 42.824 Å (MOF-C30), which are similar to experimental results (MOF-C6, MOF-C10, and MOF-C16 have experimentally determined lattice parameters of 25.832, 30.292, and 34.381 Å, respectively).[13] The details on simulation methods and crystal data of Mg- and Be-MOFs are shown in the Supporting Information. Since cubic crystalline Mg- and Be-MOFs considered herein have not, to date, been experimentally reported, their structures would be rather speculative. However, our RI-MP2 calculations show that the substitution of Zn metal sites with Mg or Be does not change the basic configuration of the $OM_4O_{12}(CH)_6$ cluster (details are given in the the Supporting Information). Density functional calculations revealed that Mg- and Be-MOF-C6 have positive elastic constants and lattice parameters (25.667 Å for Mg-MOF-C6 and 24.009 Å for Be-MOF-C6) that are similar to those determined herein (25.419 Å for Mg-MOF-C6 and 23.600 Å for Be-MOF-C6), thus indicating the stability of the crystals.[35] Thus, MOFs considered herein would be readily synthesized experimentally.

Figure 2 shows H_2 uptake capacities of Zn-MOFs at 77 and 300 K with pressures of 0.1–100 bar. Our simulations find that the H_2 uptake of Zn-MOF-C6 at 77 K and 1 bar is 1.28 wt %, which compares well with the experimental result of 1.32 wt %. For MOF-C10, we calculate 1.62 wt % compared with the experimental value of 1.50 wt %.[16] Furthermore, we calculate that MOF-C6 has 4.17 and 4.89 wt % uptake at pressures of 20 and 50 bar and 77 K,[24] which are close to the experimental results of approximately 4.7 and 5.2 wt % under the same conditions.

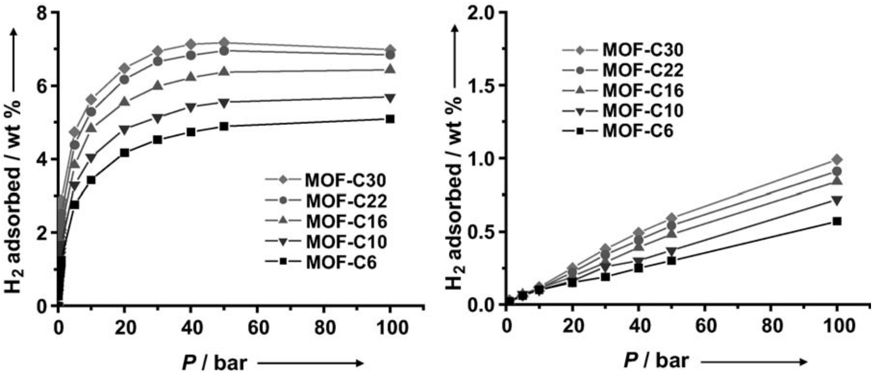

Figure 2. Predicted H_2 isotherms for Zn-MOF systems at 77 K (left) and 300 K (right).

Figure 2 shows that MOF-C30 leads to the highest uptake of H_2. Thus, at 77 K and 20 and 50 bar, the Zn-MOF-C30 system leads to an H_2 uptake of 6.47 and 7.17 wt %, respectively. At 77 K and 1 bar, we find 1.28 wt % for Zn-MOF-C6 and 2.89 wt % for Zn-MOF-C30. But at 300 K, we find that the H_2 uptake of Zn-MOF-C30 drops to 0.3 wt % at 20 bar. Therefore, we recommend larger organic linkers to achieve higher amounts of adsorbed H_2.

We also considered optimizing the metal oxide nodes. Using RI-MP2 QM calculations, we found that $Be_4O(CO_2)_6$ and $Mg_4O(CO_2)_6$ have structures similar to $Zn_4O(CO_2)_6$ but with less mass. These lighter metals improve the hydrogen storage capabilities, as shown in Figure 3 and Table 2. Thus, at 77 K and 20 bar Mg-MOF-C6 yields 6.42 wt % and Be-MOF-

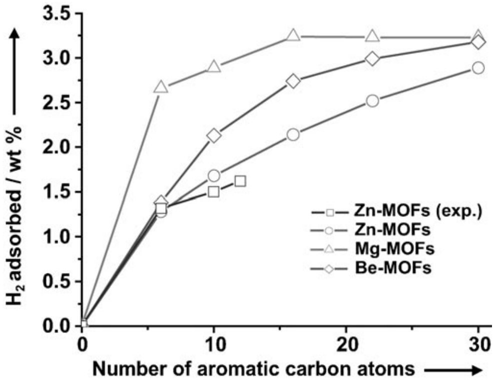

Figure 3. Hydrogen storage predicted from GCMC simulations at 77 K and 1 bar for MOFs with various metal oxide nodes and organic linkers. Experimental data are from reference [16].

Table 2: Hydrogen storage (wt %) at 77 and 300 K with a pressure of 20 bar for various MOFs.

System	T [K]	MOF-C6	MOF-C10	MOF-C22	MOF-C30
Zn-MOF	77	4.17	4.82	6.17	6.47
	300	0.15	0.16	0.22	0.25
Mg-MOF	77	6.42	7.20	7.99	8.08
	300	0.24	0.27	0.31	0.33
Be-MOF	77	6.27	6.88	7.52	7.61
	300	0.21	0.24	0.30	0.31

C6 yields 6.27 wt % uptake compared to 4.17 wt % for Zn-MOF-C6. Similarly, Mg-MOF30 yields 8.08 wt % and Be-MOF-C30 yields 7.61 wt % uptake compared to 6.47 wt % for Zn-MOF30. This result exceeds the best MOF system studied experimentally (MOF-177), which had an uptake of approximately 6.1 wt % at 77 K and 20 bar.[24]

Inelastic neutron scattering experiments for Zn-MOF-C6 as a function of H_2 loading show that the favored binding site is near the metal clusters, while increased loading leads to additional molecules occupying sites closer to the organic linkers.[13,27,28] This finding is consistent with our GCMC simulations, which at 77 K and 0.05 bar show H_2 adsorbed only near the metal oxide unit (Figure 4 a), while at higher loading (Figure 4 b) H_2 starts occupying sites on organic linkers. This result is also supported by our MP2 calculations, which indicate that the H_2 binding energy is higher with the Zn oxide cluster than with the benzene ring (Table 1). Thus, for Zn-MOF-C6, although the metal oxide cluster is preferentially responsible for the adsorption at very low pressure (H_2 loading), the importance of the organic linker is enhanced with increased H_2 loading. For example, at a pressure of 30 bar, the organic linker accounts for 74 % of the loading. On the other hand, Zn-MOF-C30 shows a different H_2 adsorption mechanism. At 77 K and 0.05 bar, H_2 is adsorbed only on the organic linkers (Figure 4 c), while at 0.5 bar it occupies sites both on the organic linkers and near the Zn oxide nodes (Figure 4 d, where H_2 adsorbed at the metal oxide nodes are shown as green atoms in the expanded view). Thus, for Zn-MOF-C30 at 1 bar and 77 K, the organic linker dominates the H_2 adsorption, with the ZnO_4 cluster playing a lesser role.

For both Mg-MOFs and Be-MOFs, we find an H_2 adsorption mechanism similar to Zn-MOFs, with the most favored site of H_2 adsorption in Mg- and Be-MOF-C6 at the vertices of the inorganic metal oxide. But for Mg and Be-MOF-C30, we find substantial H_2 storage at sites on the organic linkers. According to our simulation, the dominant hydrogen adsorption site at high pressures is on the organic linkers; thus, the higher hydrogen storage capacity of Mg- and Be-MOFs at high pressure is due solely to the ligher atomic mass of the metals.

Frost et al.[36] recently reported GCMC simulations using the Lennard–Jones empirical force field. They find that at low pressure (0.1 bar) the hydrogen uptake in Zn-MOFs correlates with the heat of adsorption, while at pressures above 30 bar the uptake correlates better with the specific surface area and specific free volume. Their results are similar to our simulations on Zn-MOF-C6, C10, and C16 in that an increased number aromatic rings in the organic linker increases the heat of adsorption of hydrogen, thud leading to higher H_2 uptake at low pressure (0.1 bar). With increased pressure, they and we both find that the H_2 uptake increases from MOF-C6 to MOF-C30, since MOF-C30 has the largest surface area and free volume. However, the simulations of Frost et al. greatly overestimate the H_2 uptake at high pressure.[36] For example, experimental results indicate that Zn-MOF-C6 stores approximately 4.8 wt % H_2 at 77 K and 90 bar,[24] in good agreement with our simulations of about 4.9 wt %, while Frost et al. predict an H_2 uptake of around 10.0 wt % at these conditions,[36] thus overestimating by more than a factor of two the free volume of H_2 uptake at high pressure.

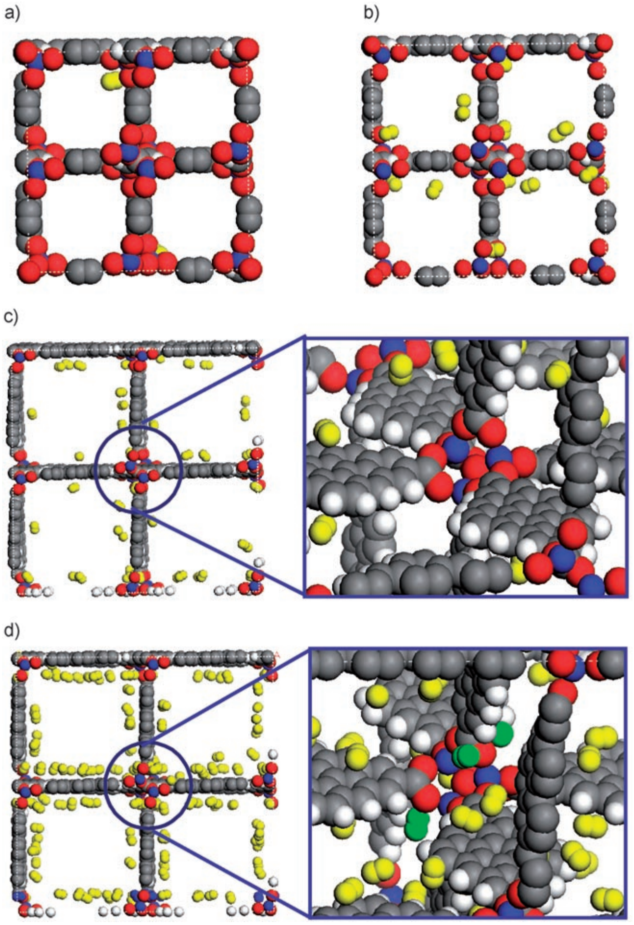

Figure 4. Snapshots of the structures of different MOFs with adsorbed H_2 at different pressures. a) Zn-MOF-C6 at $P = 0.05$ bar; b) Zn-MOF-C6 at $P = 0.5$ bar; c) Zn-MOF-C30 at $P = 0.05$ bar; d) Zn-MOF-C30 at $P = 0.5$ bar. Zn blue, O red, C gray, H white and yellow. In the expanded view of (d), H_2 adsorbed near the Zn–O vertices is shown in green.

As mentioned above, we recommend larger aromatic organic linkers to achieve higher hydrogen uptake. The larger organic linkers make the material more like a pillared graphene in which the sheets are separated by 13.0 Å (for Zn-MOF-C6). Indeed, exposing the latent edges of the six-membered rings leads to significant enhancement of specific surface area,[14] which results in higher hydrogen uptake in MOFs than in graphene.

In summary, our GCMC simulation with FFs determined from our RI-MP2 calculations gives a good reproduction of experimentally determined loading. The MOF can be improved by increasing the aromatic content of the organic linkers and by replacing Zn with Mg. At a pressure of 20 bar, the Mg-MOF-C30 proposed herein achieves 8.08 wt% storage at 77 K and 0.33 wt% at 300 K. This value is the highest among the MOF data reported to date. It is three times higher than the performance of pure carbon nanotubes and porous carbon materials. Moreover, H_2 adsorption mechanisms of MOFs can be modified by changing the aromatic organic linkers.

Received: January 22, 2007

Keywords: beryllium · hydrogen storage · magnesium · metal–organic frameworks · zinc

---

[1] L. Schlapbach, A. Zuttel, *Nature* **2001**, *414*, 353, and references therein.
[2] A. M. Seayad, D. M. Antonelli, *Adv. Mater.* **2004**, *16*, 765.
[3] D. K. Ross, *Vacuum* **2006**, *80*, 1084.
[4] C. Liu, Y. Y. Fan, M. Liu, H. T. Cong, H. M. Cheng, M. S. Dresselhaus, *Science* **1999**, *286*, 1127.
[5] Y. Ye, C. C. Ahn, C. Witham, B. Fultz, J. Liu, A. G. Rinzler, D. Colbert, K. A. Smith, R. E. Smalley, *Appl. Phys. Lett.* **1999**, *74*, 2307.
[6] W. Q. Deng, X. Xu, W. A. Goddard, *Phys. Rev. Lett.* **2004**, *92*, 166103.
[7] S. S. Han, H. M. Lee, *Carbon* **2004**, *42*, 2169.
[8] S. S. Han, H. S. Kim, K. S. Han, J. Y. Lee, H. M. Lee, J. K. Kang, S. I. Woo, A. C. T. van Duin, W. A. Goddard, *Appl. Phys. Lett.* **2005**, *87*, 213113.
[9] C. C. Tang, Y. Bando, X. Ding, S. Qi, D. Golberg, *J. Am. Chem. Soc.* **2002**, *124*, 14550.
[10] S. S. Han, J. K. Kang, H. M. Lee, A. C. T. van Duin, W. A. Goddard, *J. Chem. Phys.* **2005**, *123*, 114704.
[11] H. Lee, J. Lee, D. Y. Kim, J. Park, Y. T. Seo, H. Zeng, I. L. Moudrakovski, C. I. Ratcliffe, J. A. Ripmeester, *Nature* **2005**, *434*, 743.
[12] M. Eddaoudi, J. Kim, N. L. Rosi, D. Vodak, J. Wachter, M. O'Keeffe, O. M. Yaghi, *Science* **2002**, *295*, 469.
[13] N. L. Rosi, J. Eckert, M. Eddaoudi, D. T. Vodak, J. Kim, M. O'Keeffe, O. M. Yaghi, *Science* **2003**, *300*, 1127.
[14] H. K. Chae, D. Y. Siberio-Perez, J. Kim, Y.-B. Go, M. Eddaoudi, A. J. Matzger, M. O'Keeffe, O. M. Yaghi, *Nature* **2004**, *427*, 523.
[15] X. Zhao, B. Xiao, A. J. Fletcher, K. M. Thomas, D. Bradshaw, M. J. Roesseinsky, *Science* **2004**, *306*, 1012.
[16] J. L. C. Rowsell, A. R. Millward, K. S. Park, O. M. Yaghi, *J. Am. Chem. Soc.* **2004**, *126*, 5666.
[17] E. Y. Lee, M. P. Suh, *Angew. Chem.* **2004**, *116*, 2858; *Angew. Chem. Int. Ed.* **2004**, *43*, 2798.
[18] B. Panella, M. Hirscher, *Adv. Mater.* **2005**, *17*, 538.
[19] S. S. Kaye, J. R. Long, *J. Am. Chem. Soc.* **2005**, *127*, 6506.
[20] M. Jacoby, *Chem. Eng. News* **2005**, *83* (34), 42 (Cover story).
[21] N. L. Rosi, J. Kim, M. Eddaoudi, B. Chen, M. O'Keeffee, O. M. Yaghi, *J. Am. Chem. Soc.* **2005**, *127*, 1504.
[22] S. S. Kaye, J. R. Long, *J. Am. Chem. Soc.* **2005**, *127*, 6506.
[23] J. L. C. Rowsell, O. M. Yaghi, *Angew. Chem.* **2005**, *117*, 4748; *Angew. Chem. Int. Ed.* **2005**, *44*, 4670.
[24] A. G. Wong-Foy, A. J. Matzger, O. M. Yaghi, *J. Am. Chem. Soc.* **2006**, *128*, 3494.
[25] Y. Li, R. T. Yang, *J. Am. Chem. Soc.* **2006**, *128*, 8136.
[26] Turbomole package, University of Karlsruhe, Germany; http://www.ipc.uni-karlsruhe.de/tch/tch1/index.de.html; The calculation details are given in the Supporting Information.
[27] J. L. C. Rowsell, E. C. Spencer, J. Eckert, J. A. K. Howard, O. M. Yaghi, *Science* **2005**, *309*, 1350.
[28] T. Yildirim, M. R. Hartman, *Phys. Rev. Lett.* **2005**, *95*, 215504.
[29] J. L. C. Rowsell, J. Eckert, O. M. Yaghi, *J. Am. Chem. Soc.* **2005**, *127*, 14904.
[30] E. C. Spencer, J. A. K. Howard, G. J. McIntyre, J. L. C. Rowsell, O. M. Yaghi, *Chem. Commun.* **2006**, 278.
[31] T. Sagara, J. Klassen, J. Ortony, E. Ganz, *J. Chem. Phys.* **2005**, *123*, 014701.
[32] T. Sagara, J. Ortony, E. Ganz, *J. Chem. Phys.* **2005**, *123*, 214707.
[33] O. Hübner, A. Glöss, M. Fichtner, W. Klopper, *J. Phys. Chem. A* **2004**, *108*, 3019.
[34] The GCMC calculations were carried out using the sorption module of Cerius^2 (Accelrys, San Diego) with the FF described in the Supporting Information. The results reported herein are for excess H_2 uptake (see Ref. [37]).
[35] M. Fuentes-Cabrera, D. M. Nicholson, B. G. Sumpter, M. Widom, *J. Chem. Phys.* **2005**, *123*, 124713.
[36] H. Frost, T. Düran, R. Q. Snurr, *J. Phys. Chem. B* **2006**, *110*, 9565.
[37] G. Garberoglio, A. I. Skoulidas, J. K. Johnson, *J. Phys. Chem. B* **2005**, *109*, 13094.